









A radio parallax to the black hole X-ray binary MAXI J1820+070

P. Atri ¹★, J. C. A. Miller-Jones ¹★, A. Bahramian ¹★, R. M. Plotkin ^{1,2},
A. T. Deller ³, P. G. Jonker ^{4,5}, T. J. Maccarone ⁶, G. R. Sivakoff ⁷, R. Soria ^{8,9},
D. Altamirano ¹⁰, T. Belloni ¹¹, R. Fender ¹², E. Koering ¹³, D. Maitra ¹⁴, S. Markoff ¹⁵,
S. Migliari ^{16,17}, D. Russell ¹⁸, T. Russell ¹⁵, C. L. Sarazin ¹⁹, A. J. Tetarenko ²⁰ and
V. Tudose ²¹

¹International Centre for Radio Astronomy Research, Curtin University, GPO Box U1987, Perth, WA 6845, Australia

²Department of Physics, University of Nevada, Reno, NV 89557, USA

³Centre for Astrophysics and Supercomputing, Swinburne University of Technology, Mail Number H11, PO Box 218, Hawthorn, VIC 3122, Australia

⁴SRON, Netherlands Institute for Space Research, Sorbonnelaan 2, NL-3584 CA Utrecht, the Netherlands

⁵Department of Astrophysics/IMAPP, Radboud University Nijmegen, PO Box 9010, NL-6500 GL Nijmegen, the Netherlands

⁶Department of Physics, Texas Tech University, Box 41051, Science Building, Lubbock, TX 79409-1051, USA

⁷Department of Physics, University of Alberta, CCIS 4-183, Edmonton, AB T6G 2E1, Canada

⁸School of Astronomy and Space Sciences, University of Chinese Academy of Sciences, 52 Sanlihe Rd., Beijing 100864, China

⁹Sydney Institute for Astronomy, School of Physics A28, The University of Sydney, Sydney, NSW-2006, Australia

¹⁰Physics and Astronomy, University of Southampton, Southampton, Hampshire SO17 1BJ, UK

¹¹INAF - Osservatorio Astronomico di Brera, Via E. Bianchi 46, I-23807 Merate, Italy

¹²Astrophysics, Department of Physics, University of Oxford, Keble Road, Oxford OX1 3RH, UK

¹³Department of Astrophysics/IMAPP, Radboud University Nijmegen, PO Box 9010, NL-6500 GL Nijmegen, the Netherlands

¹⁴Department of Physics and Astronomy, Wheaton College, Norton, MA 02766, USA

¹⁵Astronomical Institute ‘Anton Pannekoek’, University of Amsterdam, Science Park 904, NL-1098XH Amsterdam, the Netherlands

¹⁶XMM–Newton Science Operations Centre, ESAC/ESA, Camino Bajo del Castillo s/n, Urb. Villafranca del Castillo, E-28691 Villanueva de la Cañada, Madrid, Spain

¹⁷Institute of Cosmos Sciences, University of Barcelona, Martí i Franquès 1, E-08028 Barcelona, Spain

¹⁸Center for Astro, Particle and Planetary Physics, New York University Abu Dhabi, PO Box 129188, Abu Dhabi, UAE

¹⁹Department of Astronomy, University of Virginia, 530 McCormick Road, Charlottesville, VA 22904, USA

²⁰East Asian Observatory, 660 N. Aōhoku Place, University Park, Hilo, HI 96720, USA

²¹Institute for Space Sciences, Atomistilor 409, PO Box MG-23, 077125 Bucharest-Magurele, Romania

Accepted 2020 January 15. Received 2020 January 14; in original form 2019 December 9

ABSTRACT

Using the Very Long Baseline Array and the European Very Long Baseline Interferometry Network, we have made a precise measurement of the radio parallax of the black hole X-ray binary MAXI J1820+070, providing a model-independent distance to the source. Our parallax measurement of (0.348 ± 0.033) mas for MAXI J1820+070 translates to a distance of (2.96 ± 0.33) kpc. This distance implies that the source reached (15 ± 3) per cent of the Eddington luminosity at the peak of its outburst. Further, we use this distance to refine previous estimates of the jet inclination angle, jet velocity, and the mass of the black hole in MAXI J1820+070 to be $(63 \pm 3)^\circ$, $(0.89 \pm 0.09) c$, and $(9.2 \pm 1.3) M_\odot$, respectively.

Key words: astrometry – parallaxes – stars: black holes – radio continuum: transients – X-rays: binaries – high angular resolution.

1 INTRODUCTION

The distances to astronomical systems are essential quantities that allow us to draw a connection between observed and physical

parameters (e.g. flux and luminosity, angular, and physical speeds). In particular, for black hole X-ray binaries (BHXBs) the relation between different accretion phases and Eddington luminosity fractions can then be studied (Maccarone 2003), and the systems can be accurately placed on the X-ray/radio luminosity plane (Gallo, Degenaar & van den Eijnden 2018) to probe jet/accretion coupling. With accurate distances, we can break the degeneracy between the inclination angles of radio jets and their speeds (Fender 2003).

* E-mail: pikky.atri@postgrad.curtin.edu.au (PA), james.miller-jones@curtin.edu.au (JCAM-J), arash.bahramian@curtin.edu.au (AB)

A well-constrained inclination angle can also help in obtaining accurate mass estimates of the black hole (BH) from the mass function of the system (Cantrell et al. 2010). An accurate distance helps in obtaining a well-constrained three-dimensional space velocity and hence the potential kick velocity (PKV) distribution of the system (Atri et al. 2019), providing clues as to the BH formation mechanism (Nelemans, Tauris & van den Heuvel 1999).

Distances to BHXBs are often estimated by studying the optical/infrared spectra of the donor star (Jonker & Nelemans 2004). The proper motion of the receding and approaching jets can also be used to place an upper limit on the distance of the BHXBs (Mirabel & Rodríguez 1994). Lower limits on the distance can be estimated by measuring either the interstellar extinction (Zdziarski et al. 1998, 2004) or the velocities of H I absorption (e.g. Chauhan et al. 2019) towards the source. X-ray dust scattering halo has also been used to constrain the distance to some the BHXBs (e.g. Xiang et al. 2011). However, these methods are all model dependent, involving certain assumptions. The only model-independent method of distance determination is measuring a high-significance trigonometric parallax. However, given their typical distances (several kpc), such high-precision observations can only be carried out using Very Long Baseline Interferometry (VLBI) or by satellites like *Gaia* (Gaia Collaboration 2018; Gandhi et al. 2019). The *Gaia*'s capabilities to conduct high-precision astrometry of BHXBs in the Galactic plane can be limited due to high extinction and low optical brightness outside of outburst. *Gaia* also has a global zero-point offset in its parallax measurements, the magnitude of which is still under debate (Chan & Bovy 2019). Therefore, targeted VLBI astrometry campaigns on outbursting BHXBs remain crucial. Of the ~ 60 BHXB candidates (Tetarenko et al. 2016), only V404 Cyg (Miller-Jones et al. 2009), Cyg X-1 (Reid et al. 2011; Gaia Collaboration 2018), and GRS 1915+105 (Reid et al. 2014) have a directly measured parallax at $>5\sigma$ significance.

In 2018 March (MJD 58188), the BHXB MAXIJ1820+070 (ASASSN-18ey, hereafter MAXIJ1820) went into outburst and was detected as a bright X-ray (Kawamuro et al. 2018) and optical (Tucker et al. 2018) transient. Archival photographic plates show two past outbursts in 1898 and 1934 (Grindlay et al. 2012), suggesting an outburst recurrence time-scale of ~ 40 yr for this source (Kojiguchi et al. 2019). In its 2018 March outburst, the transient made a complete hard (until MJD 58303.5) to soft (MJD 58310.7–58380.0) to hard state (from MJD 58393.0) outburst cycle (Shidatsu et al. 2019). Radio observations during and after the transition from hard to soft state revealed an apparently superluminal approaching jet (Bright et al. submitted). The source almost faded to quiescence in 2018 February (Russell, Baglio & Lewis 2019), enabling optical spectroscopic studies (Torres et al. 2019) to dynamically confirm the presence of a BH. It subsequently showed two reflares beginning on MJD 58552 and MJD 58691, which each lasted a couple of months (Ulowitz, Myers & Patterson 2019; Zampieri et al. 2019).

The PKV distribution of MAXIJ1820 is loosely constrained as it was based on the *Gaia* proper motion measurement $\mu_\alpha \cos \delta = -3.14 \pm 0.19$ mas yr $^{-1}$ and $\mu_\delta = -5.9 \pm 0.22$ mas yr $^{-1}$ and broad limits on the distance (1.7–3.9 kpc; Atri et al. 2019). The distance inferred from the *Gaia* parallax depended heavily on the priors used to invert the parallax (2.1–7.2 kpc; Gandhi et al. 2019). Thus, to obtain a more accurate parallax of MAXIJ1820, we carried out a targeted VLBI campaign while the source was in the hard X-ray spectral state, emitting steady compact radio jets.

2 OBSERVATIONS AND DATA REDUCTION

We monitored MAXIJ1820 (see Table 1) with the Very Long Baseline Array (VLBA), using both the Jet Acceleration and Collimation Probe of Transient X-ray Binaries (JACPOT-XRB) programme (e.g. Miller-Jones et al. 2012, 2019, proposal code BM467), and a long-running astrometry programme (e.g. Atri et al. 2019, proposal code BA130), supplemented with a targeted European VLBI Network (EVN) campaign (proposal code EA062). All observations used a combination of J1821+0549 (J1821 hereon) and J1813+065 (J1813 hereon) as the phase reference and astrometric check sources. The calibrator positions were taken from the Radio Fundamental catalogue (rfc2015a¹). Our assumed positions (J2000) were RA = 18^h21^m27.305837, Dec = 05°49′10″.65156 for J1821, and RA = 18^h13^m33.411619, Dec = 06°15′42″.03366 for MAXIJ1813. We imaged the calibrated data and determined the target position by fitting a point source in the image plane for every epoch.

2.1 VLBA campaigns

In the hard state at the start and end of an outburst, the radio jets are compact and ideal for astrometry. We took four epochs (2018 March, October, November, and December) of observations via the JACPOT-XRB program in which the first three epochs (proposal codes BM467A, BM467O, and BM467R) were observed at 15 GHz. These observations used J1813 (1.93° away from MAXIJ1820) as the phase calibrator (being brighter at 15 GHz), and cycled every ~ 2 min between it and the target, observing the check source J1821 (1.39° away from MAXIJ1820) once every eight cycles. We observed geodetic blocks (Reid et al. 2009) for half an hour at the beginning and end of each observation to better model the troposphere. The data were correlated using DiFX (Deller et al. 2011) and standard calibration steps were followed using the Astronomical Image Processing System (AIPS 31DEC17; Greisen 2003). As the source faded in 2018 December, we took the final epoch in the more sensitive 5 GHz band with the observing scheme J1821–J1813–MAXIJ1820.

We also observed under the astrometry program BA130 during its 2019 August reflare. We cycled through all these sources at 5 GHz for 1.5 h, and then at 15 GHz for 2.5 h, with geodetic blocks at the start and end of the observation. We followed standard calibration techniques within AIPS (31DEC17). MAXIJ1820 was phase referenced separately to J1821 and J1813. Data from the Mauna kea dish were removed for the complete duration of BA130B due to very high dispersive delays that were calculated by the task TECOR.

2.2 Parallax campaign: EVN data

We were also approved to observe with the EVN at 5 GHz during the expected peaks of parallax offset in RA in the months of March and September, and in declination in the months of June and December. The source was observed in 2018 October, 2018 December, and 2019 March, but faded below the detection capability of the EVN before the scheduled 2019 June epoch. J1821 was chosen as the phase reference source due to its close proximity to MAXIJ1820 and was observed every 4 min, with J1813 used as a check source. The data were reduced using AIPS (31DEC17). We used the bandpass, a

¹http://astrogeo.org/vlbi/solutions/rfc_2015a/rfc_2015a_cat.html

Table 1. Summary of the observations of MAXI J1820+070. The observing bandwidth was 32 MHz for both the VLBA and the EVN. We give the measured target positions for each epoch. When both J1813 and J1821 were observed as phase calibrators, we give target positions phase referenced to 1821. The error bars denote the statistical errors in the position measurement of the targets.

Project code	MJD	Array	Frequency (GHz)	Phase calibrator	Check source	RA (J2000) (18 ^h 20 ^m)	Dec (J2000) (07°11′)	Peak intensity (mJy bm ⁻¹)
BM467A	58193.65	VLBA	15	J1813	J1821	21 ^h 9386536(1)	07. [″] 170025(4)	31.6 ± 0.2
BM467O	58397.01	VLBA	15	J1813	J1821	21 ^h 9384875(4)	07. [″] 166302(10)	5.84 ± 0.08
EA062A	58407.71	EVN	5	J1821	J1813	21 ^h 9384883(33)	07. [″] 166075(27)	1.55 ± 0.05
BM467R	58441.73	VLBA	15	J1813	J1821	21 ^h 9384770(9)	07. [″] 165549(31)	0.56 ± 0.03
EA062B	58457.04	EVN	5	J1821	J1813	21 ^h 938437(16)	07. [″] 16485(12)	0.16 ± 0.03
BM467S	58474.86	VLBA	5	J1821, J1813	J1813, J1821	21 ^h 938462(14)	07. [″] 16498(41)	0.13 ± 0.02
EA062C	58562.25	EVN	5	J1821	J1813	21 ^h 9384324(12)	07. [″] 163533(10)	3.86 ± 0.05
BA130B	58718.06	VLBA	5	J1821, J1813	J1813, J1821	21 ^h 9382958(8)	07. [″] 160872(21)	4.09 ± 0.05
	58718.14	VLBA	15	J1821, J1813	J1813, J1821	21 ^h 9383011(3)	07. [″] 160709(14)	4.32 ± 0.12
BA130C	58755.04	VLBA	5	J1821, J1813	J1813, J1821	21 ^h 9382761(28)	07. [″] 159845(93)	1.00 ± 0.05
	58755.12	VLBA	15	J1821, J1813	J1813, J1821	21 ^h 9382730(22)	07. [″] 160090(74)	1.20 ± 0.12

priori amplitude, and parallactic angle corrections produced by the EVN pipeline, and corrected for ionospheric dispersive delays. We then performed phase, delay, and rate calibration using standard procedures in AIPS and extrapolated the phase and delay solutions derived from J1821 to both J1813 and MAXI J1820.

2.3 Mitigating systematic astrometric biases

To mitigate against systematic errors arising from low elevations, we removed all data below 20° in elevation. We also removed half an hour of data around the sunrise/sunset times at each station when the ionosphere could be changing rapidly. To prevent source structure sampled with differing uv -coverage from affecting our astrometry, we made global models of the two phase reference sources by stacking all EVN data at 5 GHz, and all VLBA data at each of 5 and 15 GHz. These global models were used to derive our final phase and delay solutions for each epoch, which were then extrapolated to MAXI J1820 and the relevant check source.

The JACPOt-XRB program (see Section 2.1) and the EVN parallax campaign (see Section 2.2) observed different extragalactic sources as phase calibrators. Hence, we scheduled the BHXb astrometry program observations (BA130B and BA130C; see Section 2.1) such that MAXI J1820 could be independently phase referenced to both J1813 and J1821. Combining these two observations with BM467S (which also cycled between all three sources), we measured an average shift of $+0.29 \pm 0.08$ mas in RA and $+0.05 \pm 0.02$ mas in Dec in the position of MAXI J1820 when it was phase referenced to J1813 as compared to when it was phase referenced to J1821. To account for this astrometric frame shift, we shifted the target positions measured when phase referenced to J1813 by -0.29 ± 0.08 and -0.05 ± 0.02 mas in RA and Dec, respectively.

To estimate the systematics arising from the troposphere ($\sigma_{\text{sys, trop}}$), we used the simulations of Pradel, Charlot & Lestrade (2006) for both the VLBA and EVN measurements, as appropriate for our target-phase calibrator angular separation and target declination. To this, we added in quadrature a conservative estimate of the ionospheric systematics (Reid et al. 2017), taken as $\sigma_{\text{sys, ion}} = 50 \mu\text{as} \left(\frac{\nu}{6.7 \text{ GHz}}\right)^{-2} \left(\frac{\theta}{1^\circ}\right)$, where ν is the observing frequency and θ is the angular separation between target and phase reference calibrator. The rms of the position of our check source (J1821 for BM467A, BM467O, BM467R, and J1813 for the remaining data sets) was in all cases less than the conservative upper limits calculated from the combined effect of $\sigma_{\text{sys, trop}}$ and $\sigma_{\text{sys, ion}}$.

Table 2. The results of the Bayesian fitting algorithm. Here we report the median and 68 per cent confidence interval from the posterior distributions of the fitted parameters.

Parameter	Value
RA ₀	18 ^h 20 ^m 21 ^s 9384568 ± 0.0000024
Dec ₀	07°11′07″.1649624 ± 0.0000680
$\mu_\alpha \cos \delta$ (mas yr ⁻¹)	-3.051 ± 0.046
μ_δ (mas yr ⁻¹)	-6.394 ± 0.075
π (mas)	0.348 ± 0.033
α_s (mas)	-0.04 ± 0.04
δ_s (mas)	0.04 ± 0.08

3 RESULTS AND ANALYSIS

3.1 A Bayesian approach for parallax fitting

To derive the proper motion ($\mu_\alpha \cos \delta$, μ_δ), parallax (π), and reference position (RA₀, Dec₀) of MAXI J1820, we fit the position as a function of time (e.g. Loinard et al. 2007), with a reference date equivalent to the mid-point of the observing campaign (MJD 58474). To perform the fit, we adopted a Bayesian approach, using the PYMC3 python package (Salvatier, Wiecki & Fonnesbeck 2016) to implement a Hamilton Markov chain Monte Carlo (MCMC; Neal 2012) technique with a No-U-Turn Sampler (NUTS; Hoffman & Gelman 2011). The *Gaia* DR2 proper motion and parallax measurements were used as priors in the procedure. We had observations at 5 and 15 GHz and so fit for any potential core shift in the calibrator peak emission from 5 to 15 GHz (α_s , δ_s), and used a flat prior from -1 to 1 mas for both α_s and δ_s . We checked for convergence in our MCMC using the Gelman–Rubin diagnostic (Gelman & Rubin 1992). The posterior distributions for all parameters are Gaussian, and the median and the 68 per cent confidence interval of each of the fitted parameters are given in Table 2. All error bars reported hereafter are at 68 per cent confidence, unless otherwise stated. The resulting fits to the sky motion are shown in Fig. 1.

3.2 Distance from parallax

Distances inferred by inverting low-significance parallax measurements suffer from Lutz–Kelker bias and can thus be underestimated (Lutz & Kelker 1973). Thus, the use of appropriate priors is essential to obtain meaningful distances (Bailer-Jones 2015; Astraatmadja &

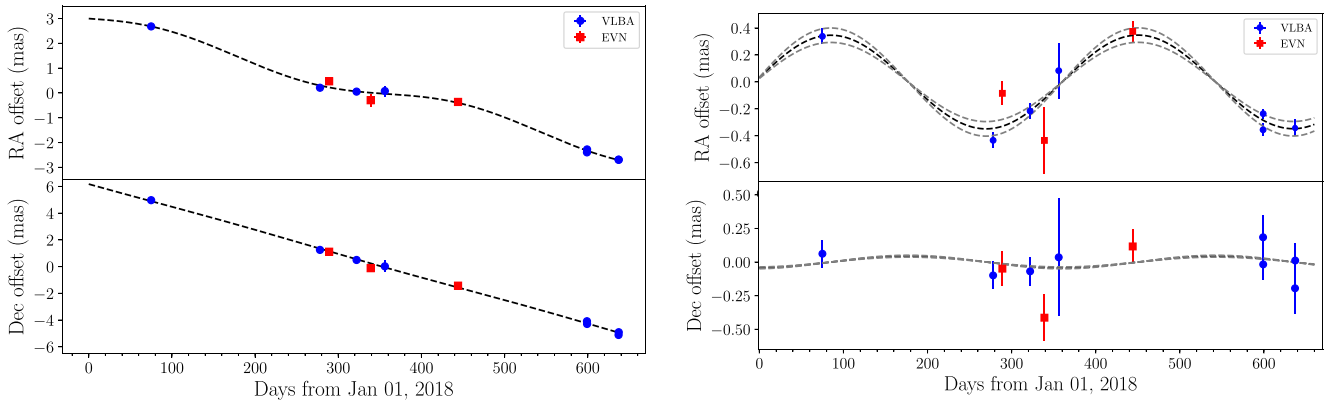


Figure 1. Astrometry of MAXIJ1820, as phase referenced to J1821 at 5 GHz. The blue circles and red squares are the positions measured by the VLBA and the EVN, respectively. All marked positions have been corrected for the frame shift due to different calibrators and frequencies. The errors bars denote the statistical and systematic errors added in quadrature. Left-hand panel: Motion in the plane of the sky relative to the fitted reference position, overlaid with the trajectory given by the best-fitting proper motion and parallax (black dashed line). Right-hand panel: Parallax signature of 0.348 (black dashed line) ± 0.033 (grey dashed lines) mas isolated by removing our best-fitting proper motion.

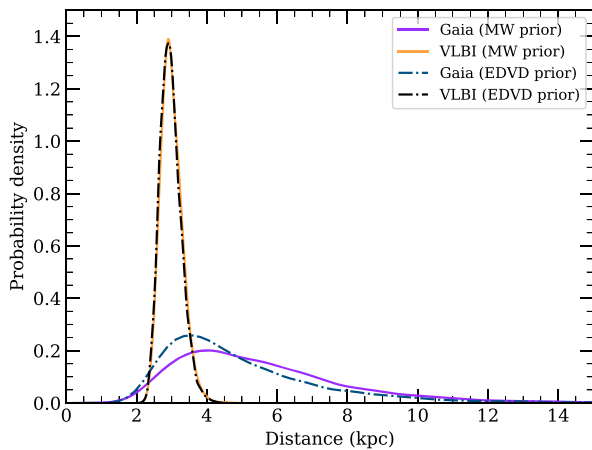


Figure 2. Distance posterior distributions of MAXIJ1820, for both our new VLBI and the *Gaia* DR2 parallax measurement. The *Gaia* DR2 distance posterior has a higher median value for the Milky Way (MW) prior (5.1 ± 2.7 kpc) than for the exponentially decreasing volume density (EDVD) prior (4.4 ± 2.4 kpc), whereas our VLBI distance distribution (2.96 ± 0.33 kpc) is insensitive to the prior chosen.

Bailer-Jones 2016). We use a prior that models the X-ray binary density distribution in the Milky Way (MW prior hereon; Atri et al. 2019) to estimate the distance posterior distribution for MAXIJ1820. With our new and more precise parallax measurement (0.348 ± 0.033 mas) and the MW prior, we determined the distance posterior distribution (Fig. 2), finding a median of 2.96 kpc and a 68 per cent confidence interval of ± 0.33 kpc. We compared this distance posterior distribution to that obtained using the parallax measurement made by *Gaia* DR2, which gave a larger median value and a wider distribution (5.1 ± 2.7 kpc). The mode and the 68 per cent higher density interval values (Bailer-Jones 2015) of this distribution are $4.13^{+2.57}_{-1.5}$ kpc. We also tested an exponentially decreasing volume density (EDVD) prior (Bailer-Jones 2015) using the scaling length parameter L for BHXBs from Gandhi et al. (2019) and find that unlike the *Gaia* DR2 distance posterior distribution (median of 4.4 ± 2.4 kpc; mode of $3.46^{+2.13}_{-1.06}$ kpc), our new distance measurement is unaffected by the chosen prior (see Fig. 2). This

shows that the high significance of our parallax measurement has led to a model-independent distance to the source.

4 DISCUSSION

With our much improved distance measurement for MAXIJ1820, we now consider the physical implications of our result.

4.1 Transition and peak outburst luminosities

The main outburst of MAXIJ1820 was observed to have a peak X-ray flux of $(14 \pm 1) \times 10^{-8}$ erg cm $^{-2}$ s $^{-1}$ in the 1–100 keV band (Shidatsu et al. 2019). A distance of 2.96 ± 0.33 kpc implies that the system only reached $0.15 \pm 0.03 L_{\text{Edd}}$ at the peak of its outburst, where L_{Edd} is the Eddington luminosity for a $10 M_{\odot}$ BH (see Section 4.3). The soft-to-hard state transition luminosity, from a flux of $(2.5 \pm 0.4) \times 10^{-8}$ erg cm $^{-2}$ s $^{-1}$, implies that the system made this transition at 3 ± 1 per cent L_{Edd} , in agreement with the average luminosity fraction of 1.58 ± 0.93 per cent L_{Edd} for BHXBs (Vahdat Motlagh, Kalemci & Maccarone 2019; Maccarone 2003). Thus, for MAXIJ1820 the state transition luminosity provides a good distance indicator.

4.2 Jet parameters

Assuming intrinsic symmetry, the measured proper motions of corresponding approaching and receding jet ejecta along with a distance can be used to uniquely determine the jet speed and inclination angle between the jet and the line of sight (Mirabel & Rodríguez 1994; Fender et al. 1999), via $\beta \cos i = \frac{\mu_{\text{app}} - \mu_{\text{rec}}}{\mu_{\text{app}} + \mu_{\text{rec}}}$, $\tan i = \frac{2d}{c} \frac{\mu_{\text{app}} \mu_{\text{rec}}}{\mu_{\text{app}} - \mu_{\text{rec}}}$, where β is the velocity of the jet (normalized to the speed of light c), μ_{app} and μ_{rec} are the proper motions of the approaching and receding components of the jet, respectively, i is the inclination angle of the jet to the line of sight, and d is the distance to the system. Bright et al. (2020) measured the proper motions of corresponding jet ejecta event during the transition phase of MAXIJ1820 $\mu_{\text{app}} = 77 \pm 1$ mas d $^{-1}$, $\mu_{\text{rec}} = 33 \pm 1$ mas d $^{-1}$. We use this with our distance constraint to estimate $\beta = 0.89 \pm 0.09$ and $\theta = (63 \pm 3)^{\circ}$.

4.3 Implications for BH mass

Torres et al. (2019) conducted optical spectroscopy on MAXI J1820 and reported a mass function of $f(M) = \frac{(M_1 \sin i)^3}{(M_1 + M_2)^2} = 5.18 \pm 0.15 M_\odot$, where $f(M)$ is the mass function, i is the inclination angle, and M_1 and M_2 are the masses of the BH and its companion, respectively. Assuming a mass ratio $q \equiv M_2/M_1 = 0.12$, they constrained the inclination angle to be $69^\circ < i < 77^\circ$, and the BH mass to be $7\text{--}8 M_\odot$. Using our derived inclination angle of $(63 \pm 3)^\circ$, we re-calculated the BH mass to be $(9.2 \pm 1.3) M_\odot$. Torres et al. (2019) suggested that the value $q = 0.12$ needs confirmation, so we also calculated the mass of the BH for the full suggested range of q (0.03–0.4) to be $(10 \pm 2) M_\odot$. We used this updated inclination angle (i) and distance (D) to estimate the inner disc radius in the high/soft state, $R_{\text{in}} = 77.9 \pm 1.0 \frac{D}{3 \text{ kpc}} \frac{\cos i}{\cos 60^\circ}$ km (Shidatsu et al. 2019). Equating this to the innermost stable orbit of the BH, we suggest that the BH in MAXI J1820 is likely slowly spinning (Steiner, McClintock & Narayan 2013).

4.4 PKV

The velocity distribution of BHBs at Galactic plane crossing has been used to determine the potential kick the system might have received at the birth of the BH (Atri et al. 2019), which is an indicator of the birth mechanism of the BH (Nelemans et al. 1999; Fragos et al. 2009; Janka 2017). A robust PKV distribution requires good constraints on the proper motion, systemic radial velocity, and the distance to the system. We used the parallax and proper motion measured in this work, combined with the systemic radial velocity of $(-21.6 \pm 2.3) \text{ km s}^{-1}$ (Torres et al. 2019) to determine a PKV distribution with a median of 120 km s^{-1} , and 5th and 95th percentiles of 95 and 150 km s^{-1} , respectively. This velocity is higher than the typical velocity dispersion of stars in the Galaxy (50 km s^{-1} ; Mignard 2000) and suggests that the system likely received a strong kick at birth, consistent with formation in a supernova explosion.

5 CONCLUSIONS

We report a precise VLBI parallax measurement of (0.348 ± 0.033) mas to the BHB MAXI J1820. Using this parallax and a Bayesian prior, we inferred a distance of (2.96 ± 0.33) kpc. We showed that MAXI J1820 reached (15 ± 3) per cent L_{Edd} at the peak of its outburst. We constrained the jet inclination angle and velocity to be $(63 \pm 3)^\circ$ and $(0.89 \pm 0.09)c$, respectively. We also report an updated BH mass estimate of $(9.2 \pm 1.3) M_\odot$, and suggest the BH is slowly spinning and likely received a strong natal kick.

ACKNOWLEDGEMENTS

We would like to thank J. S. Bright for allowing us to use their work prior to publication that helped us uniquely solve for the jet parameters in Section 4.2. The National Radio Astronomy Observatory is a facility of the National Science Foundation operated under cooperative agreement by Associated Universities, Inc. The EVN is a joint facility of independent European, African, Asian, and North American radio astronomy institutes. Scientific results from data presented in this publication are derived from the following EVN project code(s): EA062. e-VLBI research infrastructure in Europe is supported by the European Union Seventh Framework

Programme (FP7/2007–2013) under grant agreement number RI-261525 NEXPREs. JCAM-J is the recipient of an Australian Research Council Future Fellowship (FT140101082), funded by the Australian government. PGJ acknowledges funding from the European Research Council under ERC Consolidator Grant agreement no. 647208. GRS acknowledges support from a NSERC Discovery Grant (RGPIN-06569-2016). DA acknowledges support from the Royal Society. TDR acknowledges support from a Netherlands Organisation for Scientific Research (NWO) Veni Fellowship. VT is supported by programme Laplas VI of the Romanian National Authority for Scientific Research.

REFERENCES

- Astraatmadja T. L., Bailer-Jones C. A. L., 2016, *ApJ*, 832, 137
 Atri P. et al., 2019, *MNRAS*, 489, 3116
 Bailer-Jones C. A. L., 2015, *PASP*, 127, 994
 Bright J. S. et al., 2020, *Nat. Astron.*, in press
 Cantrell A. G. et al., 2010, *ApJ*, 710, 1127
 Chan V. C., Bovy J., 2019, preprint (arXiv:1910.00398)
 Chauhan J. et al., 2019, *MNRAS*, 488, L129
 Deller A. T. et al., 2011, *PASP*, 123, 275
 Fender R. P., 2003, *MNRAS*, 340, 1353
 Fender R. P., Garrington S. T., McKay D. J., Muxlow T. W. B., Pooley G. G., Spencer R. E., Stirling A. M., Waltman E. B., 1999, *MNRAS*, 304, 865
 Fragos T., Willems B., Kalogera V., Ivanova N., Rockefeller G., Fryer C. L., Young P. A., 2009, *ApJ*, 697, 1057
 Gaia Collaboration, 2018, *A&A*, 616, A1
 Gallo E., Degenaar N., van den Eijnden J., 2018, *MNRAS*, 478, L132
 Gandhi P., Rao A., Johnson M. A. C., Paice J. A., Maccarone T. J., 2019, *MNRAS*, 485, 2642
 Gelman A., Rubin D. B., 1992, *Stat. Sci.*, 7, 457
 Greisen E. W., 2003, in Heck A., ed., *Astrophysics and Space Science Library*, Vol. 285, Information Handling in Astronomy – Historical Vistas. Springer-Verlag, Berlin, p. 109
 Grindlay J., Tang S., Los E., Servillat M., 2012, in Griffin E., Hanisch R., Seaman R., eds, *Proc. IAU Symp. 285, New Horizons in Time Domain Astronomy*. Kluwer, Dordrecht, p. 29
 Hoffman M. D., Gelman A., 2011, preprint (arXiv:1111.4246)
 Janka H.-T., 2017, *ApJ*, 837, 84
 Jonker P. G., Nelemans G., 2004, *MNRAS*, 354, 355
 Kawamuro T. et al., 2018, *Astron. Telegram*, 11399, 1
 Kojiguchi N., Kato T., Isogai K., Nogami D., 2019, *Astron. Telegram*, 13066, 1
 Loinard L., Torres R. M., Mioduszewski A. J., Rodríguez L. F., González-Lópezlira R. A., Lachaume R., Vázquez V., González E., 2007, *ApJ*, 671, 546
 Lutz T. E., Kelker D. H., 1973, *PASP*, 85, 573
 Maccarone T. J., 2003, *A&A*, 409, 697
 Mignard F., 2000, *A&A*, 354, 522
 Miller-Jones J. C. A., Jonker P. G., Dhawan V., Brisken W., Rupen M. P., Nelemans G., Gallo E., 2009, *ApJ*, 706, L230
 Miller-Jones J. C. A. et al., 2012, *MNRAS*, 421, 468
 Miller-Jones J. C. A. et al., 2019, *Nature*, 569, 374
 Mirabel I. F., Rodríguez L. F., 1994, *Nature*, 371, 46
 Neal R. M., 2012, preprint (arXiv:1206.1901)
 Nelemans G., Tauris T. M., van den Heuvel E. P. J., 1999, *A&A*, 352, L87
 Pradel N., Charlot P., Lestrade J.-F., 2006, *A&A*, 452, 1099
 Reid M. J., Menten K. M., Brunthaler A., Zheng X. W., Moscadelli L., Xu Y., 2009, *ApJ*, 693, 397
 Reid M. J., McClintock J. E., Narayan R., Gou L., Remillard R. A., Orosz J. A., 2011, *ApJ*, 742, 83
 Reid M. J., McClintock J. E., Steiner J. F., Steeghs D., Remillard R. A., Dhawan V., Narayan R., 2014, *ApJ*, 796, 2
 Reid M. J. et al., 2017, *AJ*, 154, 63

- Russell D. M., Baglio M. C., Lewis F., 2019, *Astron. Telegram*, 12534, 1
- Salvatier J., Wiecki T. V., Fonnesbeck C., 2016, *PyMC3*, *Astrophysics Source Code Library*, record ascl:1610.016
- Shidatsu M., Nakahira S., Murata K. L., Adachi R., Kawai N., Ueda Y., Negoro H., 2019, *ApJ*, 874, 183
- Steiner J. F., McClintock J. E., Narayan R., 2013, *ApJ*, 762, 104
- Tetarenko B. E., Sivakoff G. R., Heinke C. O., Gladstone J. C., 2016, *ApJS*, 222, 15
- Torres M. A. P., Casares J., Jiménez-Ibarra F., Muñoz-Darias T., Armas Padilla M., Jonker P. G., Heida M., 2019, *ApJ*, 882, L21
- Tucker M. A. et al., 2018, *ApJ*, 867, L9
- Ulowetz J., Myers G., Patterson J., 2019, *Astron. Telegram*, 12567, 1
- Vahdat Motlagh A., Kalemci E., Maccarone T. J., 2019, *MNRAS*, 485, 2744
- Xiang J., Lee J. C., Nowak M. A., Wilms J., 2011, *ApJ*, 738, 78
- Zampieri L., Munari U., Ochner P., Manzini F., 2019, *Astron. Telegram*, 12747, 1
- Zdziarski A. A., Poutanen J., Mikolajewska J., Gierlinski M., Ebisawa K., Johnson W. N., 1998, *MNRAS*, 301, 435
- Zdziarski A. A., Gierliński M., Mikołajewska J., Wardziński G., Smith D. M., Harmon B. A., Kitamoto S., 2004, *MNRAS*, 351, 791

This paper has been typeset from a $\text{\TeX}/\text{\LaTeX}$ file prepared by the author.